

however, since some of the experimental data necessary for a reanalysis have not yet been published and since further experiments of the same type are now in progress.

If we accept the combined result for α_3 , then we may obtain a value for α_1 of 0.170η . Since the errors on α_1 and α_3 are related, it is not appropriate to present the phase shifts in the form $\alpha_1 \pm \Delta\alpha_1$, $\alpha_3 \pm \Delta\alpha_3$. Figure 5 shows the results of the π^+p and π^-p experiments plotted in the α_1/η vs α_3/η plane. The intersection of the

solid lines gives the best estimate of α_1 and α_3 and the ovals are contours of equal probability for other combinations of α_1 and α_3 .

VII. ACKNOWLEDGMENTS

We are indebted to Dr. Irwin Pless for many valuable suggestions and for assistance during the operation of the bubble chamber. We also wish to thank Mr. M. Pyka and Mr. N. Campbell for their help in scanning and analyzing the pictures.

Pion-Proton Scattering at 220 Mev*

J. ASHKIN, J. P. BLASER,[†] F. FEINER,[‡] AND M. O. STERN[§]
Carnegie Institute of Technology, Pittsburgh, Pennsylvania

(Received October 8, 1956)

Pion-proton differential scattering cross sections have been measured at 220 ± 7 Mev. Measurements were made at eight angles using scintillation counters and a liquid hydrogen target. Statistical errors range from 5 to 10%. Phase shift analyses have been made of the data in the customary manner. No evidence for *d*-wave scattering has been found.

INTRODUCTION

IN a recent article¹ we reported on experiments at Carnegie Institute of Technology to measure the angular distribution of negative and positive pions of 150 and 170 Mev scattered in hydrogen. It was found, in agreement with earlier results obtained by Fermi and his co-workers at Chicago, that the data could be analyzed on the assumptions that charge independence was valid in meson-nucleon interactions, and that only *s* and *p* waves were strongly scattered. Since it was interesting to see at what point *d*-wave scattering could no longer be neglected, we decided to do an accurate differential scattering experiment with pions of the highest energy for which the yield in our cyclotron is sufficient. This energy turned out to be 220 Mev and this paper presents the results of the investigation. Measurements at nearly the same energy (217 Mev) have been reported by workers^{2,3} at the University of Chicago; the agreement is good. Our corrected cross section values are summarized in Table I. In Table IV we present two sets of phase shifts which give a good fit to our data.

* Research partially supported by the U. S. Atomic Energy Commission.

[†] Now at Observatoire Cantonal, Neuchatel, Switzerland.

[‡] Now at Knolls Atomic Power Laboratory, Schenectady, New York.

[§] Now at General Atomic, San Diego, California.

¹ Ashkin, Blaser, Feiner, and Stern, Phys. Rev. **101**, 1149 (1956), hereafter referred to as I.

² M. Glicksman, Phys. Rev. **94**, 1334 (1954).

³ H. Taft, Phys. Rev. **101**, 1116 (1956).

EXPERIMENTAL PROCEDURE

For details on the internally produced negative meson beam, scattering geometry, scintillation counters, hydrogen target, electronics, and experimental procedure, the reader is referred to I.

It had previously been found⁴ that for practical purposes the positive pion beam had an upper energy limit of 195 Mev. To extend this limit, an externally produced positive pion beam was used. The arrangement is shown in Fig. 1. A bundle of protons coming out of the cyclotron is focused horizontally by a wedge magnet onto a carbon target 1.5 in. by 3 in. in cross

TABLE I. Experimental cross sections in the center-of-mass system at 220 Mev, in mb sterad⁻¹. Errors shown include statistical and angle-dependent uncertainties, but do not include an over-all uncertainty in the scale of the cross sections amounting to 5% for the negative pion cross sections and 4% for the positive pion cross sections. $\sigma_\gamma(\theta)$ is the differential cross section for detecting either of the two γ rays resulting from decay of the neutral pion produced in charge-exchange scattering. $\sigma_-(\theta)$ and $\sigma_+(\theta)$ refer to the elastic scattering of negative and positive pions respectively.

$\theta_{c.m.}$	$\sigma_+(\theta)$	$\sigma_-(\theta)$	$\sigma_\gamma(\theta)$
37°	18.6±1.1	2.55±0.15	7.55±0.22
52°	15.5±0.9	1.68±0.11	6.51±0.22
70°	9.3±0.8	1.16±0.09	4.70±0.23
90°	5.8±0.7	0.92±0.09	3.71±0.24
110°	6.1±0.8	1.10±0.10	4.11±0.31
128°	9.3±0.9	1.33±0.12	4.95±0.32
143°	14.0±1.1	1.99±0.15	5.23±0.41
162.5°	16.2±1.5	2.60±0.28	6.55±0.57

⁴ Ashkin, Blaser, Feiner, Gorman, and Stern, Phys. Rev. **96**, 1104 (1954).

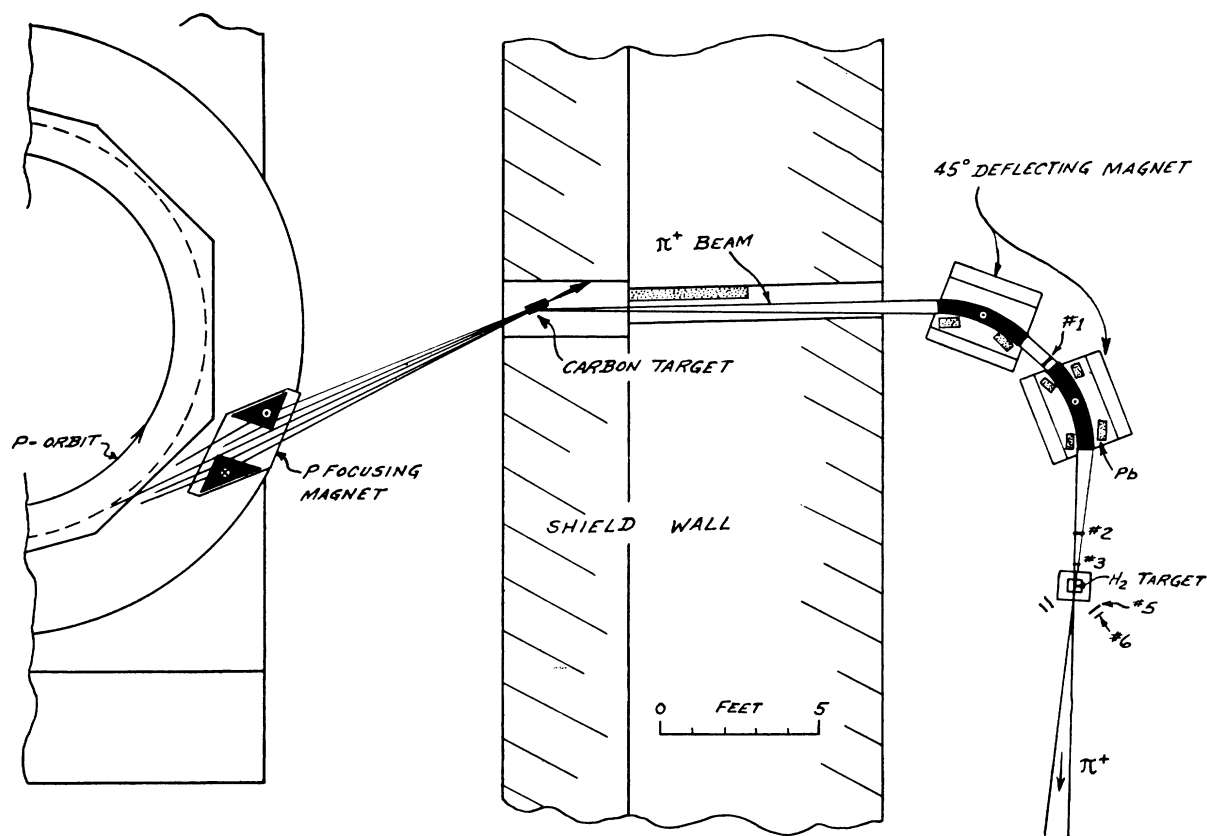


FIG. 1. Experimental arrangement for the π^+ measurements, showing proton-focusing magnet, external carbon target, meson-deflecting magnets, and detecting apparatus. Counters 1, 2, and 3 form the monitor with time-of-flight discrimination. Two telescopes incorporating two counters (5,6) each detect scattered pions.

section located near the entrance to the shielding wall. Some pions produced at around 30° proceed through the channel in the shielding into the experimental area. Here two 45° bending magnets separate the positive pions from the negative ones, electrons and most muons and protons, and bring the beam to a crude focus in the neighborhood of the liquid hydrogen target. By varying the current in the magnets, pions of varying energies can be obtained.

As the energy is increased, the π^+ beam is found to be increasingly contaminated by protons of the same stiffness. The first of the three monitor counters is therefore placed between the two deflecting magnets, thereby affording about 2 meters of time-of-flight discrimination against the much slower protons. The detecting counters and geometry for positive pions are the same as in I. In this manner a beam of about $30 \pi^+$ mesons per second was obtained at 220 Mev.

Both positive and negative pion beams contained about 5% muon contamination. The beam energy and spread, 220 ± 7 Mev, were determined from analysis of range curves.

Differential scattering measurements were carried out in the same manner as in I. Copper absorbers preceded the elastic scattering detectors at small angles

to stop recoiling protons. Suitable allowance was made for pion absorption in the copper. Gamma rays from charge-exchange scattering were detected by counting the electrons produced by the gamma rays in a $\frac{1}{4}$ -inch lead converter.

In addition we measured the total π^- cross section in hydrogen by transmission.

PROCESSING OF DATA

A detailed discussion of the necessary corrections to the data is contained in I. The same applies to the determination of the efficiency of the gamma-ray conversion telescope. Uncertainty in the absolute efficiency contributes a major part of the indeterminacy in absolute value of the π^- cross sections, estimated as 5%.

Table I gives the experimental differential cross sections in the center-of-mass system after the corrections have been applied. $\sigma_-(\theta)$ and $\sigma_+(\theta)$ are the differential cross sections for elastic scattering of π^- and π^+ mesons, respectively, and $\sigma_\gamma(\theta)$ is the differential cross section for detecting either of the two gamma rays resulting from decay of the π^0 meson produced in charge-exchange scattering. A theoretical correction for interference between the nuclear and Coulomb

TABLE II. Correction for Coulomb interference. Addition to the experimental elastic scattering cross sections ($\pi^- \rightarrow \pi^-$ and $\pi^+ \rightarrow \pi^+$) of Table I gives the purely nuclear scattering cross sections. The correction is different for the two sets of phase shifts (i) and (ii) of Table IV.

$\theta_{c.m.}$	Correction (mb/sterad)			
	Set (i)		Set (ii)	
	$\pi^- \rightarrow \pi^-$	$\pi^+ \rightarrow \pi^+$	$\pi^- \rightarrow \pi^-$	$\pi^+ \rightarrow \pi^+$
37°	0.07	-0.44	0.06	-0.44
52°	0.02	-0.19	0.04	-0.19
70°	0.00	-0.08	0.03	-0.08
90°	-0.01	-0.03	0.02	-0.03
110°	-0.01	0.00	0.02	0.00
128°	-0.02	0.01	0.02	0.01
143°	-0.02	0.02	0.01	0.02
162.5°	-0.02	0.02	0.01	0.02

scattering amplitudes as described in I is not yet included (see below).

The errors given in Table I have been obtained by combining the statistical counting errors with the uncertainties in the angle-dependent corrections at the different angles. An additional over-all uncertainty in the scale of the cross sections, amounting to 5% for the π^- cross sections and 4% for the π^+ cross sections, is not included in the quoted errors.

The angular distributions for the three reactions listed in Table I were analyzed for a least squares fit to the form $a + b \cos\theta + c \cos^2\theta$. From the nine coefficients a , b , c , a graphical phase shift analysis⁵ was made, yielding scattering phase shifts of the Fermi type in the neighborhood of those given in Table IV. Two sets, (i) and (ii), were obtained, differing mainly in the sign of the phase shift α_1 . Their properties will be discussed further below. As was done for the scattering at 150 and 170 Mev in I, these preliminary phase shifts were used to derive a theoretical correction, contained in Table II, to eliminate the effect of the Coulomb scat-

TABLE III. Least-squares analysis of the data of Table I in the form $a + b \cos\theta + c \cos^2\theta$, after correcting for Coulomb interference. a , b , and c are given in mb/sterad. Errors shown have the same meaning as in Table I. The coefficients for the π^0 angular distribution [cross section $\sigma_0(\theta)$] are obtained from those corresponding to $\sigma_\gamma(\theta)$ by the method of Fermi (reference 6). σ is the integrated cross section for each process in mb. A measure of the goodness of fit is given by the quantity M , having the expectation value 5.

Phase shift set	Cross section	a	b	c	σ	M
(i)	$\sigma_+(\theta)$	5.86 ± 0.48	3.93 ± 0.62	16.06 ± 1.27	140.9 ± 4.2	3.1
	$\sigma_-(\theta)$	0.86 ± 0.06	0.30 ± 0.08	2.07 ± 0.18	19.5 ± 0.6^a	6.0
	$\sigma_\gamma(\theta)$	3.87 ± 0.16	1.30 ± 0.18	4.31 ± 0.39	66.6 ± 1.3^a	3.5
	$\sigma_0(\theta)$	1.23 ± 0.13	0.88 ± 0.12	4.26 ± 0.39	33.3 ± 0.7	...
(ii)	$\sigma_-(\theta)$	0.89 ± 0.06	0.28 ± 0.08	2.06 ± 0.18	19.8 ± 0.6^b	5.8
Coefficients for the remaining reactions are the same as for set (i)						

^a The π^- total cross section as measured by transmission is 53.7 ± 1.5 mb. After correction for the radiative capture reaction ($\pi^- + p \rightarrow n + \gamma$ estimated to have 0.6 mb total cross section) and for Coulomb interference (requiring an estimated addition of 0.1 mb), the total π^- cross section is 53.2 ± 1.5 mb. The error quoted is the total error.

^b Because of the different Coulomb correction associated with the phase shift set (ii), the corrected total cross section in this case is 53.5 ± 1.5 mb.

⁵ J. Ashkin and S. Vosko, Phys. Rev. **91**, 1248 (1953).

tering amplitude. Application of this correction to the experimental elastic scattering cross sections of Table I in principle gives the purely nuclear scattering, but the result depends on the particular set of phase shifts chosen. The sign of the correction has been taken to agree with the observation of Taft³ that the Coulomb interference for π^+ scattering at small angles is constructive at 217 Mev. The correction is appreciable for the forward scattering angles. Figure 2 gives the

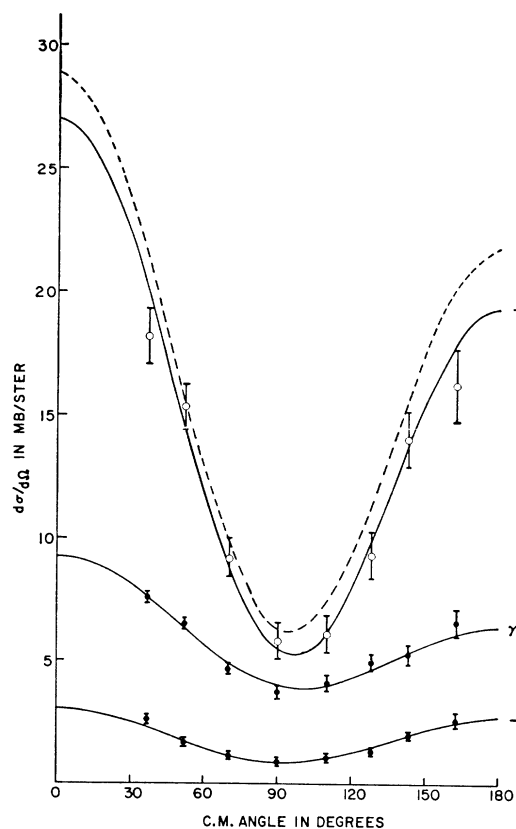


FIG. 2. 220-Mev pion-proton differential cross sections. The experimental points represent the cross-section values of Table I after Coulomb correction using set (i) of Table II. The solid curves give the cross sections corresponding to the phase shift set (i) of Table IV. The dotted curve represents the sum of elastic and charge-exchange differential cross sections for negative pions (multiplied by 3) as taken from the least-squares coefficients a , b , and c corresponding to $\sigma_-(\theta)$ and $\sigma_0(\theta)$ of Table III. The difference between the dotted curve and the π^+ cross section is proportional to the differential scattering cross section for isotopic spin $\frac{1}{2}$; see Eq. (1) of text.

differential center-of-mass cross sections $\sigma_+(\theta)$, $\sigma_-(\theta)$, and $\sigma_\gamma(\theta)$ corrected for the Coulomb interference according to the phase shift set (i).

A final least-squares analysis of the angular distributions was made based on the cross sections corrected for the Coulomb effect. The resulting coefficients a , b , c are listed in Table III for each of the two types of phase shift sets. A noticeable difference between the two cases was obtained only for the elastic π^- scattering. The coefficients for the π^0 angular distribution in charge-

exchange scattering [cross section $\sigma_0(\theta)$] are obtained from those corresponding to the angular distribution of the decay gamma rays [cross section $\sigma_\gamma(\theta)$] by the method first proposed by Fermi.⁶

The total cross sections σ obtained by integration of the angular distributions are given in the next to last column of Table III. In the case of π^- we have also measured the total cross section by transmission with the result given in the footnotes to Table III. The requirement that there be agreement between the π^- cross sections obtained by transmission and by integration was important for the determination of the absolute gamma-ray detection efficiency. Comparison with other total cross-section measurements^{2,7,8} in this energy range shows satisfactory agreement.

The last column of Table III gives the quantity $M = \sum \epsilon_i^2$, where the ϵ_i are the deviations of the experimental points from the least squares fit, measured in units of the experimental error. Since there are eight angles and three constants, M has the expectation value 5. From the values obtained it is clear that the inclusion of a d wave, equivalent to the addition of terms $d \cos^3\theta + e \cos^4\theta$ to our polynomial representing the cross sections, cannot lead to a significant improvement in fit. Thus no positive evidence for d -wave scattering has been found at 220 Mev.

Before proceeding to the analysis of the scattering in terms of the phase shifts for the different states of angular momentum and isotopic spin, it is worth remarking that the isotopic spin dependence can in principle be extracted directly from the differential cross sections themselves. On the assumption that the total isotopic spin is conserved by the pion-nucleon interaction, it is easy to verify that

$$3 \left\{ \frac{d\sigma(-)}{d\Omega} + \frac{d\sigma(0)}{d\Omega} \right\} = \frac{d\sigma(3/2)}{d\Omega} + 2 \frac{d\sigma(1/2)}{d\Omega} = \frac{d\sigma(+)}{d\Omega} + 2 \frac{d\sigma(1/2)}{d\Omega}, \quad (1)$$

where the $(-)$, (0) , and $(+)$ refer to the elastic scattering of π^- , charge-exchange scattering of π^- , and elastic scattering of π^+ , respectively, and the $(3/2)$ and $(1/2)$ refer to the scattering in isotopic spin states $\frac{3}{2}$ and $\frac{1}{2}$, respectively. Although the $\frac{3}{2}$ and $\frac{1}{2}$ amplitudes interfere in the elastic and charge scattering of π^- taken separately, the interference terms drop out in the sum. Comparison of the "total" differential cross section for negative pions (multiplied by 3) with the differential cross section for positive pions therefore indicates the differential scattering in the state with isotopic spin $\frac{1}{2}$.

⁶ Anderson, Fermi, Martin, and Nagle, Phys. Rev. **91**, 155 (1953).

⁷ S. J. Lindenbaum and L. C. L. Yuan, Phys. Rev. **100**, 306 (1955).

⁸ Ignatenko, Mukhin, Ozerov, and Pontecorvo, Zhur. Eksptl. i Teoret. Fiz. **30**, 7 (1956).

TABLE IV. Phase shifts representing the pion scattering at 220 Mev. Notation is that of Fermi (reference 6). See the text for explanation of the alternative sets (i) and (ii).

Phase shift	Set (i)	Set (ii)
α_3	-14.5°	-18°
α_{33}	112°	112°
α_{31}	-5°	0°
α_1	15°	-8.5°
α_{13}	-5°	11.5°
α_{11}	7°	3°

This comparison is made in Fig. 2. The dotted curve represents the left-hand side of Eq. (1) as taken from the least squares coefficients a, b, c of Table III. It is clear that the $I = \frac{1}{2}$ scattering is small but definite. A similar comparison at 150 and 170 Mev (see I) shows that the $I = \frac{1}{2}$ scattering is smaller at these energies than at 220 Mev.

PHASE SHIFT ANALYSIS

The final phase shift analysis of the scattering was performed by a graphical method⁵ based on the coefficients a, b, c given in Table III. The phase shifts so obtained were then varied until we achieved by trial and error a good over-all fit to the three π^+ coefficients and the six π^- coefficients. Only "Fermi-type" phase shifts were considered. We thereby arrived at two sets of phase shifts presented in Table IV and labeled (i) and (ii), respectively. The phase shift notation is that of Fermi.⁶

In Fig. 2 the a, b, c derived from the set (i) are used to plot the solid curves which may be compared with the experimental points obtained from Table I after applying the Coulomb correction of Table II. An indication of the quality of the fit is provided by the quantity M representing the sum of squares of the deviations (in units of the errors). Since there are 24 experimental points and 6 independent phase shifts to be adjusted, M has the expectation value $24 - 6 = 18$. The actual value for the phase shift set (i) is 17. For the phase shift set (ii) M has the value 18 so that the two sets give equally good fits to the data.

The main difference between the two sets of phase shifts is in the sign of α_1 (and possibly of α_{13}). For set (ii) the s -wave phase shift α_1 is in reasonable agreement

TABLE V. Comparison of the real parts of the forward scattering amplitudes D_3 and D_1 for isotopic spins $\frac{3}{2}$ and $\frac{1}{2}$ at 220 Mev, as calculated from the dispersion relations (reference 12) and from the two sets of phase shifts of Table IV representing our measurements.

	Dispersion relations	Phase shifts	
		(i)	(ii)
D_3 ^a	-1.95	-2.05	-1.98
D_1 ^b	0.27	0.39	0.59

^a The amplitude D_3 as given here is dimensionless. $D_3 = \sin 2\alpha_3 + 2 \sin 2\alpha_{33} + \sin 2\alpha_{31}$.

^b $D_1 = \sin 2\alpha_1 + 2 \sin 2\alpha_{13} + \sin 2\alpha_{11}$.

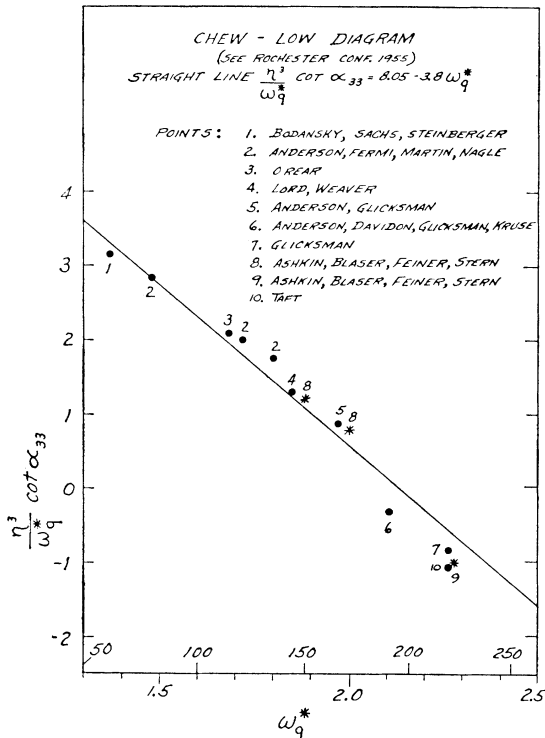


FIG. 3. Plot of $(\eta^3/\omega_q^*) \cot \alpha_{33}$ against ω_q^* (G. F. Chew and F. E. Low, reference 13). η is the center-of-mass momentum of the pion in units of μc and ω_q^* is the center-of-mass energy minus the proton rest energy in units of μc^2 . 1: Bodansky, Sachs, and Steinberger, Phys. Rev. **93**, 1367 (1954); 2: Anderson, Fermi, Martin, and Nagle, Phys. Rev. **91**, 155 (1953); 3: J. Orear, Phys. Rev. **96**, 1417 (1954); 4: J. J. Lord and A. B. Weaver (quoted by reference 12); 5: H. L. Anderson and M. Glicksman, Phys. Rev. **100**, 268 (1955); 6: Anderson, Davidon, Glicksman, and Kruse, Phys. Rev. **100**, 279 (1955); 7: M. Glicksman, Phys. Rev. **94**, 1335 (1954); 8: Ashkin, Blaser, Feiner, and Stern, Phys. Rev. **101**, 1149 (1956); 9: Point corresponding to the present experiment; 10: H. D. Taft, Phys. Rev. **101**, 1116 (1956).

with the preferred solution of de Hoffmann *et al.*⁹ according to which α_1 passes continuously from positive values below 190 Mev to negative values above. For set (i), on the other hand, α_1 maintains its positive value and increases from 150 and 170 to 220 Mev more or less linearly with meson momentum. α_3 maintains its negative value and similarly increases in size in going to 220 Mev. This behavior is in fact consistent with the linear extrapolations of Orear¹⁰: $\alpha_1 = 0.16\eta$

⁹ de Hoffmann, Metropolis, Alei, and Bethe, Phys. Rev. **95**, 1586 (1954).

¹⁰ J. Orear Phys. Rev. **96**, 176 (1954) and **100**, 288 (1955).

and $\alpha_3 = -0.11\eta$ (in radians), where η is the meson momentum in units of μc .

It is interesting to compare the two sets of phase shifts on the basis of the dispersion relations recently introduced into the discussion of meson scattering.^{11,12} The second column of Table V gives values for the quantities D_3 and D_1 calculated for laboratory energy 220 Mev from the dispersion formulas.¹² D_3 and D_1 are the real parts of the forward scattering amplitudes for isotopic spin $\frac{3}{2}$ and $\frac{1}{2}$, respectively. The third and fourth columns give the values calculated from phase shift sets (i) and (ii). The agreement with set (i) is slightly, but probably not significantly, better.

The large phase shift α_{33} is the same for both sets (i) and (ii) at 220 Mev and has passed from below to above 90° with increasing energy. This is consistent with the observed change in the forward to backward asymmetry of the positive pion scattering (favoring backward scattering at 150 Mev, and forward scattering at 220 Mev) and corresponds to a change of sign of the real part of the *p*-wave amplitude relative to the *s* wave amplitude. The corresponding change in the Coulomb interference from destructive to constructive has been observed by Taft.³

Figure 3 shows a plot of $(\eta^3/\omega_q^*) \cot \alpha_{33}$ vs ω_q^* , where η is the pion momentum in units of μc and ω_q^* is the energy in the center-of-mass system minus the proton rest energy in units of μc^2 . According to Chew and Low's cutoff meson theory,¹³ the relationship should be approximately linear. Our new point is shown, and gives reasonable agreement.

In this connection it should be mentioned that according to the cutoff theory α_{31} and α_{13} should be small, negative and equal,¹³ while α_{11} should be small and its sign negative or positive depending on whether the coupling constant is small or large.¹⁴ Friedman, Lee, and Christian,¹⁴ using an intermediate coupling method, have calculated α_{31} and α_{13} to be approximately -3° at 220 Mev while α_{11} is near $+6^\circ$. It is interesting that these are close to the values given in our phase shift set (i).

We wish to thank J. Kunze and R. McIlwain for their help in setting up the equipment and taking data.

¹¹ Goldberger, Miyazawa, and Oehme, Phys. Rev. **99**, 986 (1955).

¹² Anderson Davidon, and Kruse, Phys. Rev. **100**, 339 (1955).

¹³ G. F. Chew and F. E. Low, Phys. Rev. **101**, 1570 (1956) and *Proceedings of the Fifth Annual Rochester Conference on High-Energy Physics* (University of Rochester Press, Rochester, 1955).

¹⁴ Friedman, Lee, and Christian, Phys. Rev. **100**, 1494 (1955).